Micellar-shape anisometry near isotropic–liquid-crystal phase transitions

R. Itri and L. Q. Amaral
Instituto de Física, Universidade de São Paulo, Caixa Postal 20516, São Paulo, Brazil
(Received 8 September 1992)

Micellar phases of the sodium dodecyl (lauryl) sulfate (SLS)–water–decanol system have been studied by x-ray scattering in the isotropic (I) phase, with emphasis on the $I \rightarrow$hexagonal (H_α) and $I \rightarrow$nematic-cylindrical (N_c) lyotropic liquid-crystal phase transitions. Analysis of the scattering curves is made through modeling of the product $P(q)S(q)$, where $P(q)$ is the micellar form factor and $S(q)$ is the intermicellar interference function, calculated from screened Coulombic repulsion in a mean spherical approximation. Results show that micelles grow more by decanol addition near the $I \rightarrow N_c$ transition (anisometry $\nu \simeq 3$) than by increased amphiphile concentration in the binary system near the $I \rightarrow H_\alpha$ phase transition ($\nu \simeq 2.4$). These results compare well with recent theories for isotropic–liquid-crystal phase transitions.

PACS number(s): 05.70.Fh, 61.10.Lx, 64.70.Md, 82.70.Dd

I. INTRODUCTION

Phase diagrams of amphiphile-water systems are rather complex, involving the appearance of different forms of aggregates as a function of concentration and temperature [1]. Among lyotropic liquid-crystal phases with positional order, the more common are the lamellar (one-dimensional order) and hexagonal (two-dimensional order), considered to be of "smectic" type, when compared with thermotropic mesophases. The typical sequence of growing order with increasing amphiphile concentration is isotropic (I)–hexagonal (H_α)–lamellar (L_α), where the α symbol refers to disordered paraffin chains.

Addition of a third component enriches the polymorphism [2]. In particular, long-chain alcohols (as decanol) may promote the appearance of nematic phases, with finite anisotropic aggregates having long-range orientational order [3,4]. The isotropic-uniaxial nematic (N) transition is predicted in several models, assuming ellipsoidal and spherocylindrical finite objects [5,6].

Phase diagrams obtained from theoretical models and computer simulations were able to predict phases in the ordering sequence I–N–smectic lamellar (Sm_L)–smectic columnar (Sm_C) [7,9] as a function of particle axial ratio and particle number density. The smectic Sm_L is, however, not an L_α phase, since the former is made up of discrete objects while the latter corresponds to a rearrangement of monomers in extended bilayers. An understanding of the direct I–Sm_C phase transition has been attained only recently [10] for a system of polydisperse [11] spherocylinders of finite and small sizes.

The Sm_C phase did not seem to correspond to the H_α phase, which was viewed as made up of "infinite" cylindrical aggregates [1,2]. However, a recent study [12] of the hexagonal cell parameter a of the binary sodium dodecyl (lauryl) sulfate (SLS)–water system as a function of volume concentration c_v in the H_α domain, after a $I \rightarrow H_\alpha$ phase transition, shows the functional behavior expected for finite objects [8] ($a \propto c_v^{-1/3}$). This leads to a new description of the H_α phase: polydisperse spherocylindrical micelles with length that may be growing along the range of this phase. In H_α phases after a $N \rightarrow H_\alpha$ phase transition, a behavior typical of "infinite" cylinders ($a \propto c_v^{-1/2}$) has been observed in another system [13].

In order to get information on micellar-shape anisometry near the isotropic-lyotropic liquid-crystal phase transitions and compare it with theoretical predictions, we have performed detailed analysis of x-ray scattering curves in concentrated micellar solutions. The system chosen was SLS-water-decanol; the binary SLS-water system undergoes a $I \rightarrow H_\alpha$ transition [14,15], while the ternary system shows a $I \rightarrow$nematic cylindrical (N_c) phase transition [16]. This system is particularly suited since it is one of the most studied in isotropic micellar solutions [17–21], and its liquid-crystal phases have also received considerable attention [12,22].

II. EXPERIMENTAL SECTION

Samples were prepared with usual procedures [15]. Binary solutions were studied in the range 5 wt % to 40 wt % of SLS, the last corresponding to an H_α phase. Ternary solutions were obtained by gradual addition of decanol to a binary solution with 26.15 wt % of SLS (water:SLS molar ratio $M_w = 45.2$), until a N_c phase was obtained [16] (at decanol:SLS molar ratio $M_d = 0.286$).

Samples conditioned in sealed glass capillaries of 1-mm inside diameter were investigated by small-angle x-ray scattering at room temperature (22 ± 1 °C), using both photographic technique (transmission geometry, Cu $K\alpha$–Ni filter) and scintillation detector. Scattering curves were obtained with a small-angle Rigaku-Denki goniometer, using a line beam-transmission geometry and Cu $K\alpha$ radiation (graphite monochromator).

The scattered intensity J_{obs} was corrected by subtracting a background (parasitic scattering plus electronic noise). In general, the solvent scattering is also subtract-

ed. In our case, it is not known *a priori* the amount of water bound to the micelle and the possible variation of this amount with concentration. We have not subtracted, therefore, the water scattering from J_{obs}; the subtracted parasitic scattering consisted of the measured intensity without sample, multiplied by the sample attenuation.

III. ANALYSIS METHOD

It is well known that small-angle scattering intensity $I(q)$ of an isotropic system of monodisperse spheres (or spheroids with low anisotropy) is given by [17,23,24]:

$$I(q)=n_p P(q)S(q) ,$$

where n_p is the numeric density of particles and the scattering vector $q=4\pi \sin\theta/\lambda$. This corresponds to a separation of the intraparticle $[P(q)]$ and interparticle $[S(q)]$ interference effects. For systems with small polydispersity ($<20\%$), the deviation corresponds to a diffuse background scattering [24].

$P(q)$ is the orientational average of the particle form factor, and may be modeled according to the geometry of the particle. In our case, the micelle will be modeled in a spheroidal shape, with two shells of different electronic levels: paraffin $\rho_{par}=0.275\ e/\text{Å}^3$, and polar head ρ_{pol} (free parameter), relative to water $\rho_0=0.327\ e/\text{Å}^3$, using Eq. (3) from Ref. [25]. The shorter semiaxis R_{par} is kept fixed at 16.7 Å, which is the length of a fully extended dodecyl chain [15,26], and the longer semiaxis is νR_{par}, with ν equal to the axial ratio, a second free parameter.

The function $S(q)$ may be calculated [27] for a given micellar charge (degree of ionization α, third free parameter) by assuming the micelle to be a charged sphere, interacting through a screened Coulomb potential in the mean spherical approximation (MSA), according to the method developed by Hayter and Penfold [Eq. (13) of Ref. [27(a)]. The ellipsoid [for the $P(q)$ model] and the sphere have an equal inner-hydrocarbon-core volume and are surrounded by a polar head of an average diameter equal to 4.6 Å [28]. The structural parameters and the micellar charge are then obtained by fitting the product $P(q)S(q)$ (convoluted with the effect of incident beam height, negligible width) to the experimental curve $J_{obs}(q)$.

The use of the approximate MSA for spheroids of low anisometry has been discussed in Ref. [24b], where it has been shown that it can be affected by choosing a physically plausible effective hard-core diameter. The best is to consider the excluded volume of a rigid prolate spheroid determined by calculating the second virial coefficient. For $\nu\sim1.3$, the result is the same as one obtains for a hard sphere with volume equal to that of the spheroid. For $\nu=2$ to 3, the systematics we use, of considering a spheroid of equal volume, may lead to an overestimation of the micellar anisometry ν of about 4–6 % in $S(q)$. In the fit of $I(q)=P(q)S(q)$, the overall error is smaller, since we use $P(q)$ of the ellipsoid.

IV. RESULTS

Figure 1 shows the several scattering curves obtained by increasing the SLS concentration in the binary system.

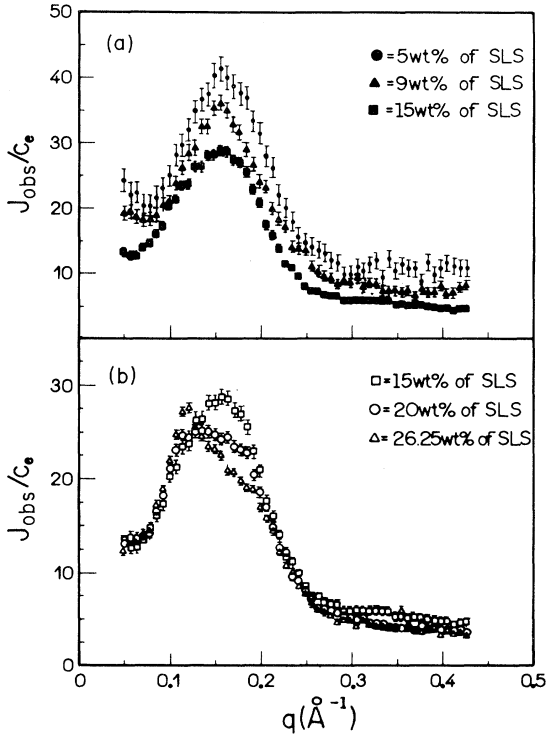

FIG. 1. Small-angle x-ray scattering curves of SLS:water solutions, normalized in relation to the electronic concentration c_e: (a) 5, 9, and 15 wt % of SLS; (b) 15, 20, and 26.25 wt % of SLS.

For concentrations up to 15 wt % of SLS, the curves [Fig. 1(a)] present a peak centered (in s^{-1}, $q=2\pi s$) at 36 Å, which does not change position with concentration—evidence that this peak is primarily related to the inner micellar structure [14,21]. For higher concentrations [Fig. 1(b)], a second peak at larger s^{-1} values starts to grow due to the interactions between micelles, becoming well defined at 26.25 w %.

Figure 2(a) presents the results for the binary system at the higher concentrations near the $I\rightarrow H_\alpha$ transition, and Fig. 2(b) for the ternary system near the $I\rightarrow N_c$ transition. The main feature is the growth of a second-order peak in the ternary system and the increase of the interparticle distance, while in the binary system a $1/\sqrt{3}$ peak appears in the photos [15].

An initial study of the I-H_α phase transition focused on intermicellar peak positions (by photographic technique, free of smearing effects) and available space for distribution of amphiphile-water moieties was performed [15]. It showed that, assuming local three-dimensional positional order, micelles have an almost constant effective radius for concentrations ≥ 15 wt % and small anisometries. Micellar growth above $\nu\sim1.5$ would imply some degree of local orientational order.

A plot of these s^{-1} intermicellar peak positions as a function of volume concentration c_v in the binary system for concentrations higher than 15 wt % is shown in Fig. 3. The fit gives $s^{-1}=32.0c_v^{-1/3}$. The $c_v^{-1/3}$ behavior is typical of almost-constant particle sizes, with interparticle distance decreasing in all three dimensions [12]. The

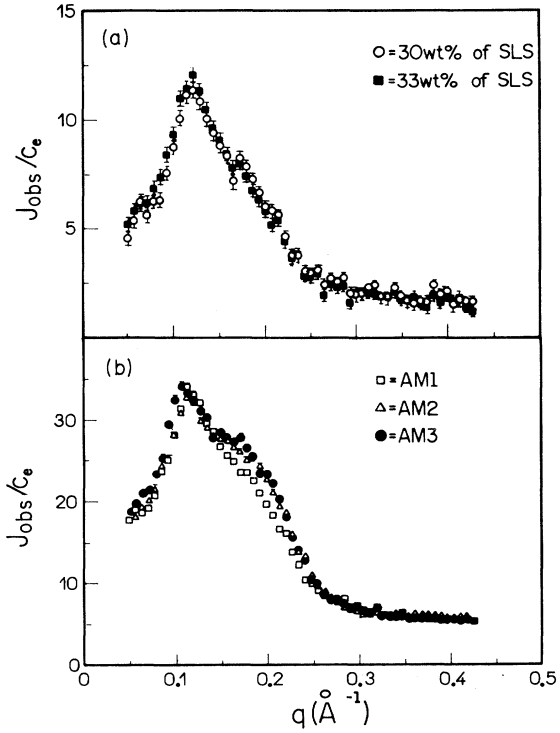

FIG. 2. Small-angle x-ray scattering curves of concentrated solutions, normalized in relation to the electronic concentration c_e: (a) 30 and 33 wt % of SLS:water binary solution; (b) ternary solution obtained by addition of decanol to a binary solution with 26.15 wt % of SLS (see Table II).

value of the coefficient of adjustment suggests that the micellar anisometry is small; the exact ν value depends on which type of short-range order is assumed [15]. This gives support to an analysis of the scattering curves in terms of spheroids of constant R_{par} and low anisometries, as in the present article.

Figure 4 shows the modeling obtained for 9 wt % of

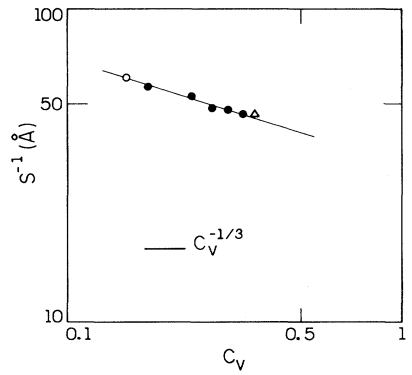

FIG. 3. Intermicellar peak position s^{-1} in the binary system as a function of volume concentration c_v, calculated using values 0.89 and 1.00 cm^3/g for SLS and water specific volumes. The value for the smallest concentration is taken from SANS data [18(b)] and the highest concentration corresponds to d_{100} of the H_α phase.

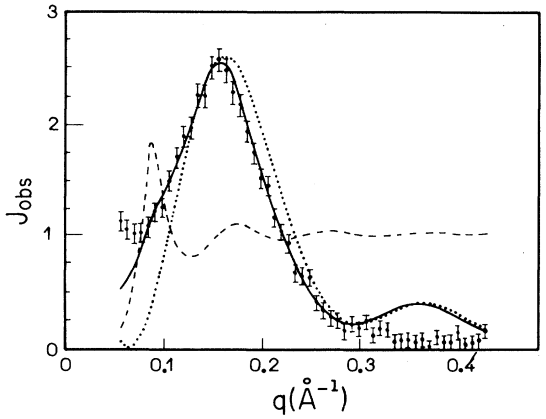

FIG. 4. Small-angle x-ray scattering curve for 9 wt % of SLS: (. . . .) $P(q)$; (— — — —) $S(q)$; the thick line is the product $P(q)S(q)$ convoluted with the smearing effect of the collimation for comparison with experimental data. Parameters of adjustment: $\nu=1.7$, $\rho_{pol}=0.4\ e/\text{Å}^3$, and $\alpha=0.28$ (see Table I).

SLS in water (similar to the 5 wt % of SLS [21]). From Fig. 4, it is seen that $S(q)$ is not negligible for small q values. Also, the maximum of $S(q)$ practically coincides with the first minimum of $P(q)$, and therefore the scattered curve is dominated by the inner micellar structure. The presence of a second peak in $P(q)$ and not in $J_{obs}(q)$

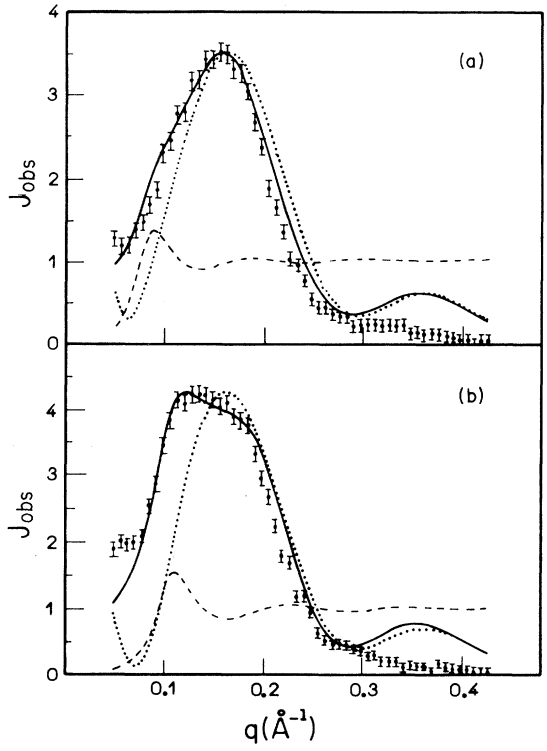

FIG. 5. Small-angle x-ray scattering curve: (. . . .) $P(q)$; (— — — —) $S(q)$; the thick line is the product $P(q)S(q)$ convoluted with the smearing effect of the collimation for comparison with experimental data. (a) 15 wt % of SLS: $\nu=3$, $\rho_{pol}=0.417\ e/\text{Å}^3$, and $\alpha=0.1$; (b) 20 wt % of SLS: $\nu=2$; $\rho_{pol}=0.41\ e/\text{Å}^3$, and $\alpha=0.16$ (see Table I).

TABLE I. Binary samples changing SLS wt %, corresponding molar concentration, and values of parameters obtained by fitting scattering curves: polar-head electronic density ρ_{pol}, spheroid anisometry ν, and effective degree of ionization α.

Φ (wt %)	$[\Phi]$ (M)	ρ_{pol} ($e/\text{Å}^3$)	ν	α
5	0.174	0.393–0.396	1.4–1.6	0.24–0.20
9	0.312	0.400–0.401	1.7–2.0	0.28–0.24
15	0.512	0.409–0.417	2.0–3.0	0.21–0.10
20	0.694	0.410–0.413	2.0–2.6	0.16–0.05
26.25	0.911	0.410	2.0–2.4	0.16–0.0
30	1.042	0.410	2.2–2.4	0.10–0.0
33	1.146	0.408	2.4	0.0

is related to polydispersity effects not considered in the model (only included as diffuse background scattering). Such effects may cause smooth oscillations in the region of high q [19a]. Table I presents the range of parameter values obtained from the fit.

For 15 and 20 wt %, it is possible to reach good adjustments within a wider range of parameter values (Table I), because both intramicellar as well as intermicellar effects influence the scattering curve. Then, greater ν values can be compensated by decreasing α values, leading to the same quality of fit. Figure 5(a) shows an example for 15 wt % and Fig. 5(b) for 20 wt % of SLS.

The peak of the intermicellar interference becomes well pronounced at higher concentrations. Figure 6(a) shows results for 26.25 wt % of SLS, while Fig. 6(b) shows the corresponding radial distribution function $g(x)$ (where $x=r/\sigma$, dimensionless unit; σ = particle diameter).

Figure 7 shows the modeling for high concentrations in the vicinity of the isotropic → liquid-crystal phase transitions: $I \rightarrow H_\alpha$ in the binary system [Fig. 7(a)] and $I \rightarrow N_c$ in the ternary system [Fig. 7(b)]. The quality of fit of the first interference peak is comparable in both curves, and assures a good definition of ν and α values. Near the transition, the fit requires $\alpha=0$ (excluded volume interaction), and thus ν values correspond to the maximum possible anisometries. The second interference peak shows a reasonable agreement in the ternary system [Fig. 7(b)], essentially because the pseudolamellar order characteristic of the N_c phase [16] is well simulated by the isotropic interference function. On the other hand, the lack of agreement of this second-order peak in the binary system [Fig. 7(a)] occurs because the intrinsically isotropic formalism for $S(q)$ is unable to account for the observed $1/\sqrt{3}$ peak. The ν value obtained near the

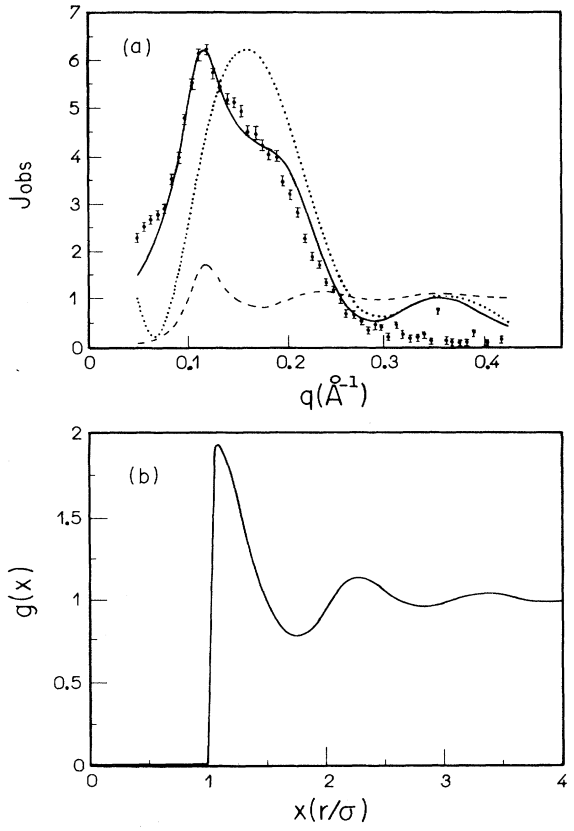

FIG. 6. (a) Small-angle x-ray scattering curve for 26.25 wt % of SLS: (· · · ·) $P(q)$; (— — — —) $S(q)$; the thick line is the product $P(q)S(q)$ convoluted with the smearing effect of the collimation for comparison with experimental data. Parameters of adjustment: $\nu=2.2$, $\rho_{pol}=0.41\ e/\text{Å}^3$, and $\alpha=0.1$ (see Table I). (b) Radial distribution function $g(x)$ corresponding to above $S(q)$. $x=r/\sigma$, dimensionless unit, σ = particle diameter.

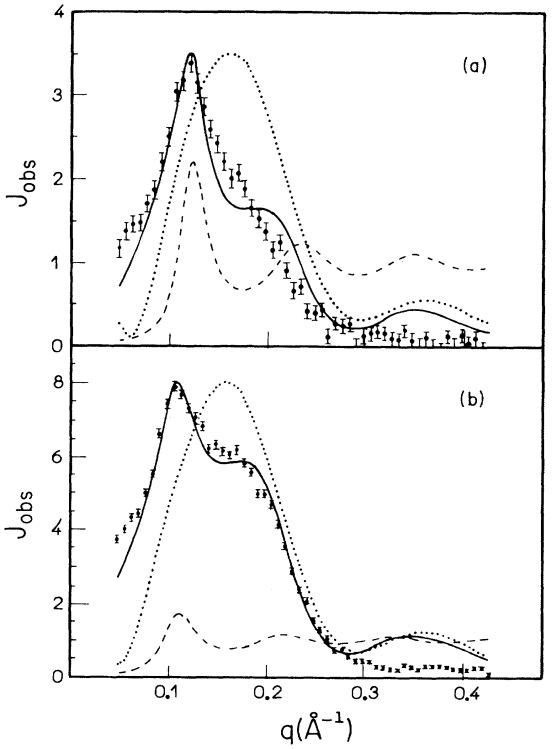

FIG. 7. Isotropic solutions near $I \rightarrow$ liquid-crystal phase transitions: (a) 33 wt % of SLS in water. Parameters of adjustment: $\nu=2.4$, $\rho_{pol}=0.408\ e/\text{Å}^3$, and $\alpha=0$ (near $I \rightarrow H_\alpha$); (b) ternary solution AM3 ($M_w=45.2$, $M_d=0.139$). Parameters of adjustment: $\nu=3$, $\rho_{pol}=0.408\ e/\text{Å}^3$, and $\alpha=0.05$ (near $I \rightarrow N_c$). For the symbols, see Tables I and II.

$I \rightarrow H_\alpha$ transition ($\nu \sim 2.4$, Table I) evidences also some degree of anisotropic short-range order [15].

V. DISCUSSION

From Table I, it is clear from the binary-system data that ν increases with concentration ($\nu \simeq 1.4$ for 5 wt % to $\nu \simeq 2.4$ for 33 wt %), indicating small micellar growth for increasing amphiphile concentration. The growth occurs essentially in the 5 to 15 wt % of the SLS interval, and there is a stabilization tendency for higher concentrations in the I phase, in agreement with previous study [15] and with the $s^{-1} \alpha c_v^{-1/3}$ behavior.

An increase in micellar length has also been obtained by analysis of small-angle neutron scattering (SANS) [17,18] using the same method, for concentration $< 0.6M$ (~ 15 wt % of SLS in water), in agreement with our results. We stress that the analysis for higher concentrations seems to have been performed previously by SANS only for the $1.042M$ solution [18a] (~ 30 wt % of SLS in water). Although our results agree in relation to micellar length, there is a small difference in α value. In the neutron analysis, the effect of counterion size on the potential leads to α values greater than those obtained by us. It should be remarked that the ionization coefficient α has to be considered an "effective value," since as a free parameter it can suppress the deficiencies of the potential assumed in this methodology.

The radial distribution function $g(x)$ [Fig. 6(b)] indicates the closeness of micelles, with $g(x)$ exhibiting a first peak at $x \simeq 1.2$. In such a case, excluded-volume interactions become fundamental [29]. So, decreases in the α value for the concentrated I phase may be indicative of the presence of other types of interactions (attractives, solvation) not considered in the model.

In the ternary solutions, we have observed micellar growth by gradual addition of decanol (Table II). An increase in the position value (s^{-1}) of the first interference peak is also observed, indicating an increase in the water layer among micelles in the shorter particle-axis direction, associated with an increase in micellar length.

It is clear from our results that micelles grow more by decanol addition near the $I \rightarrow N_c$ transition ($\nu \simeq 3$) than by increased amphiphile concentration in the binary system near the direct $I \rightarrow H_\alpha$ transition ($\nu \simeq 2.4$). We stress that this result is a significant one. The difference in ν at these two transitions is about 20%, larger than the errors that may affect ν in view of the approximate MSA used in the calculation of $S(q)$. Furthermore, eventual systematic errors due to the spherical approximation do not affect the relative result that gives larger growth at the I-N transition as compared with the I-H transition.

To determine if micellar growth occurs in the rodlike particle direction also in the ternary system, a modeling using oblate ellipsoidal shape for $P(q)$ (disclike) has been tried [30]. It was not possible to obtain good agreement between model and experimental curves in that case, and oblate micellar shapes near the $I \rightarrow N_c$ phase transition can be ruled out.

It is known that decanol tends to be localized on lower-curvature regions of micellar aggregates [31,32]. However, decanol in the studied solution does not lead yet to a flattening of the particles, but to micellar growth. This can be understood in terms of a micellar spherocylindrical model: the hemispherical caps—the greater-curvature regions—are unfavorable, with decanol promoting initially an increase in the cylindrical part.

In fact, a recent study [33] of the relative stability of spherocylindrical (sc) and prolate ellipsoidal forms in terms of bending energy showed that sc micelles are favored over prolate ellipsoids for $\nu > 1.8$. The anisometry $\nu_{sc} = L/2R$ of a spherocylinder with radius R, cylinder length l, and total length $L = l + 2R$ is related to the anisometry ν of a prolate ellipsoid of the same volume through

$$\nu_{sc} = (2\nu + 1)/3 \ .$$

From a theoretical point of view, only recently [10,11] predictions of the I-H phase transition have been reported. Previous calculations [8,9] with hard spherocylinders predicted only I-nematic-Sm$_C$ phase transitions; that is, nematic orientational ordering and/or smectic layering order of the finite cylinders always appeared before the hexagonal columnar phase. However, introduction of polydispersity in cylinder length [10,11] suppresses smectic ordering in favor of the high-concentration hexagonal phase. Moreover, the theoretical calculations of Taylor and Herzfeld [10], where rodlike aggregates are reversibly assembled via linear aggregation of n spherical monomers, indicate a direct I-H phase transition for weak aggregation, that is, when the average aggregate size is small.

TABLE II. Ternary samples changing molar ratio decanol:SLS, M_d, for a constant molar ratio water:SLS $M_w = 45.2$. Values of parameters obtained by fitting scattering curves: polar-head electronic density ρ_{pol}, spheroid anisometry ν, and effective degree of ionization α. Modeling in I phase was done with AM1, AM2, and AM3 samples; for AM4 sample, I-N_c phase coexistence was observed; N_c is the nematic cylindrical phase; s^{-1} = position value of the first interference peak obtained by photographic method.

Samples	M_d	ρ_{pol} ($e/\text{Å}^3$)	ν	α	s^{-1} (Å)
AM1	0.034	0.405	2.1–2.3	0.13–0.05	52.7±0.3
AM2	0.084	0.413	2.5–2.7	0.08–0.0	54.0±0.5
AM3	0.139	0.408	3.0	0.05	55.6±0.5
AM4	0.195				57.0±0.5
N_c	0.286				60.0±0.5

In our case, the "spherical monomer" corresponds to a "spherical micelle." The basic aspects of micellar aggregation are the same: the chemical potential of the aggregate [Eq. (16) of Ref. [10] obeys the condition required for micellar equilibrium [34]. Therefore, all results obtained by Taylor and Herzfeld [10] can be used for micelles, noting only that the average aggregation number $\langle n \rangle$ is not the amphiphile aggregation number of a micelle, but the number of spherical micelles with radius R equivalent in volume to a spherocylindrical micelle of cylinder length $l=4(n-1)R/3$, or to a spheroidal micelle with $\nu=n$.

Taylor and Herzfeld's results show that the separation between I-H and I-N-H behavior (close to c curves of Figs. 2 and 3, Ref. [10]) occurs precisely for $\langle n \rangle \sim 3$. Smaller aggregates, with $\nu<3$, lead to a direct I-H_α transition at higher concentrations, while larger aggregates, with $\nu \geq 3$, lead to a I-N transition at lower concentrations. There is very good agreement between their values of c_v and $\langle n \rangle$ at which the transitions start to occur in the I phase and our results: The SLS plus decanol volume concentration in the ternary system at I-N_c coexistence (sample AM4) is $c_v=0.265$ (calculated using the value 1.21 cm^3/g for decanol specific volume), falling between curves c and b in Fig. 3—Ref. [10]. The SLS volume concentration in the binary system at I-H_α coexistence is $c_v=0.343$ (37 wt %), falling between c and d curves in Fig. 3—Ref. [10].

The only discrepancy regards the prediction [10] of a wide (I,H) coexistence range (from 0.34, close to experimental result, to 0.60), while experimentally the H_α phase is well defined at $c_v=0.372$. This discrepancy can be attributed either to a more weakly first-order transition or to an actual micellar growth at the transition. They predict [10] at the end of the coexistence range $\langle n \rangle \sim 10$; a more marked micellar growth at the transition may shrink the coexistence region. There are therefore indications that the process of orientational-induced growth, predicted [31] for the I-N transition, occurs in a more marked and even discontinuous way at the I-H_α transition (in fact, such discontinuous growth is predicted for even smaller aggregates in curves d and e of Fig. 3—Ref. [10]).

ACKNOWLEDGMENTS

Thanks are due to FAPESP, CNPQ, and FINEP foundations for financial support.

[1] V. Luzzati, in *Biological Membranes,* edited by D. Chapman (Academic, London, 1968), Chap. 3, pp. 71–122; G. J. T. Tiddy, Phys. Rep. **57**, 1 (1980).
[2] P. Ekwall, in *Advances in Liquid Crystals,* edited by G. H. Brown (Academic, London, 1975), Vol. 1, pp. 1–142.
[3] L. Q. Amaral, C. A. Pimentel, M. R. Tavares, and J. A. Vanin, J. Phys. Chem. **71**, 2940 (1979).
[4] J. Charvolin, A. M. Levelut, and E. T. Samulski, J. Phys. Lett. **40**, L587 (1979).
[5] D. Frenkel, B. M. Mulder, and J. P. McTague, Phys. Rev. Lett. **52**, 287 (1984); D. Frenkel and B. M. Mulder, Mol. Phys. **55**, 1171 (1985); R. Holyst and A. Poniewierski, *ibid.* **68**, 381 (1989).
[6] M. Baus, J. L. Colot, X. G. Wu, and H. Xu, Phys. Rev. Lett. **59**, 2184 (1987); A. Perera, G. N. Patey, and J. J. Weis, J. Chem. Phys. **89**, 6941 (1988).
[7] A. Stroobants, H. N. W. Lekkerkerker, and D. Frenkel, Phys. Rev. A **36**, 2929 (1987); D. Frenkel, H. N. W. Lekkerkerker, and A. Stroobants, Nature **332**, 822 (1988).
[8] M. P. Taylor, R. Hentschke, and J. Herzfeld, Phys. Rev. Lett. **62**, 800 (1989); R. Hentschke, M. P. Taylor, and J. Herzfeld, Phys. Rev. A **40**, 1678 (1989).
[9] A. Poniewierski and R. Holyst, Phys. Rev. Lett. **61**, 2461 (1988); J. A. C. Veerman and D. Frenkel, Phys. Rev. A **41**, 3237 (1990); A. Poniewierski and T. J. Sluckin, *ibid.* **43**, 6837 (1991).
[10] M. P. Taylor and J. Herzfeld, Phys. Rev. A **43**, 1892 (1991).
[11] T. J. Sluckin, Liq. Cryst. **6**, 111 (1989).
[12] L. Q. Amaral, A. Gulik, R. Itri, and P. Mariani, Phys. Rev. A **46**, 3548 (1992).
[13] L. Q. Amaral, R. Itri, P. Mariani, and R. Micheletto, Liq. Cryst. **12**, 913 (1992).
[14] F. Reiss-Husson and V. Luzzati, J. Phys. Chem. **68**, 3504 (1964); J. Colloid Interface Sci. **21**, 534 (1966).
[15] R. Itri and L. Q. Amaral, J. Phys. Chem. **94**, 2198 (1990).
[16] L. Q. Amaral, M. E. M. Helene, D. R. Bittencourt, and R. Itri, J. Phys. Chem. **91**, 5949 (1987); L. Q. Amaral and M. E. M. Helene, *ibid.* **92**, 6094 (1988).
[17] (a) J. B. Hayter and J. Penfold, J. Chem. Soc. Faraday Trans. 1 **77**, 1851 (1981); (b) Colloid Polym. Sci. **261**, 1022 (1983).
[18] (a) E. Y. Sheu, C. F. Wu, and S. H. Chen, Phys. Rev. A **32**, 3807 (1985); (b) S. H. Chen, Physica (Utrecht) **137B**, 183 (1986); C. F. Wu, E. Y. Sheu, D. Bendedouch, and S. H. Chen (unpublished); E. Y. Sheu and S. H. Chen, J. Phys. Chem. **92**, 4466 (1988).
[19] (a) B. Cabane, R. Duplessix, and T. Zemb, J. Phys. (Paris) **46**, 2161 (1985); (b) T. Zemb and P. Charpin, J. Phys. (Paris) **46**, 249 (1985).
[20] V. Y. Bezzobotnov, S. Borbely, L. Cser, B. Faragö, I. A. Gladkih, Y. M. Ostanevich, and S. Vass, J. Phys. Chem. **92**, 5738 (1988); S. Borbely, L. Cser, Y. M. Ostanevich, and S. Vass, J. Phys. Chem. **93**, 7967 (1989).
[21] R. Itri and L. Q. Amaral, J. Phys. Chem. **95**, 423 (1991).
[22] (a) R. M. Wood and M. P. McDonald, J. Chem. Soc. Faraday Trans. 1 **81**, 273 (1985); (b) P. Kékicheff and B. Cabane, J. Phys. (Paris) **48**, 1571 (1987).
[23] A. Guinier and G. Fournet, *Small Angle Scattering of X-rays* (Wiley, New York, 1955).
[24] (a) D. Bendedouch and S. H. Chen, J. Phys. Chem. **87**, 1653 (1983); (b) M. Kotlarchyk and S. H. Chen, J. Chem. Phys. **79**, 2461 (1983).
[25] J. Marignan, P. Basserau, and P. J. Delord, J. Phys. Chem. **90**, 645 (1986).
[26] C. Tanford, J. Phys. Chem. **76**, 3020 (1972).
[27] (a) J. B. Hayter and J. Penfold, Mol. Phys. **42**, 109 (1981); (b) J. P. Hansen and J. B. Hayter, Mol. Phys. **6**, 651 (1982).
[28] D. Stigter, J. Phys. Chem. **68**, 3603 (1964); **79**, 1008 (1975).
[29] T. Odjik, J. Chem. Phys. **93**, 5172 (1990).

[30] R. Itri, Ph.D. Thesis, University of São Paulo, 1991.
[31] W. M. Gelbart, W. E. McMullen, and A. Ben-Shaul, J. Phys. (Paris) **46**, 1137 (1985).
[32] B. Jönsson and H. Wennerström, J. Phys. Chem. **91**, 338 (1987).
[33] G. Taddei and L. Q. Amaral, J. Phys. Chem. **96**, 6102 (1992).
[34] R. E. Goldstein, J. Chem. Phys. **84**, 3367 (1986).